

## Filament manufacturing via external grooving of an HDPE pipe wall: RSM optimization and mechanical tests validation

Sabrina Mammeri<sup>1,2,a</sup>, Khaider Bouacha<sup>2,b</sup>, Kamel Chaoui<sup>\*,1,c</sup>, Wafia Ghabeche<sup>3,d</sup>, Khaoula Berkas<sup>1,e</sup>

<sup>1</sup>Mechanics of Materials and Plant Maintenance Research Laboratory (LR3MI), Mechanical Eng. Dept., Faculty of Technology, Badji Mokhtar University, Annaba, Algeria

<sup>2</sup>Faculty of Sciences and Technology, Mohamed-Chérif Messaadia University, Souk-Ahras, Algeria

<sup>3</sup>Mechanics of Materials and Plant Maintenance Research Laboratory (LR3MI), Mechanical Eng. Dept., LR3MI, Elect. Eng. Dept., Faculty of Technology, A. Mira University of Bejaia, Algeria

Article Info	Abstract
<p><i>Article history:</i></p> <p>Received 14 Jan 2024 Accepted 12 May 2024</p> <p><i>Keywords:</i></p> <p>Polyethylene pipe; Machining; RSM optimization; Filament; Stress-strain behavior; Mechanical properties</p>	<p>In order to explore the possibilities of manufacturing and testing specimens from extruded HDPE pipes to retrace material inherent properties, continuous filaments are circumferentially machined by grooving. The proposed protocol imposes to keep to a strict minimum damage effects since semi-crystalline polyethylene is sensitive to deformation and heat. A Taguchi plan is adopted with inputs (cutting speed; feed rate; depth of cut). The modeled performance characteristics are roughness criteria (Rt; Ra) and temperature (T°). Using ANOVA and response surface methodology, the optimized values are 137.0 m/min, 0.4 mm/rev and 4.0 mm respectively for Vc, f and ap. At the highest desirability, the values of Rt (1.100 μm), Ra (0.223 μm) and T (36.44 °C) are satisfactory compared to turning data. Tensile tests on specimens from outer, middle and inner pipe show that (σ-ε) curves are reproducible with a pronounced drawing zone, especially for the inner pipe layers. Practically, the elasticity modulus is increased by 43% from outer to inner layers while the utmost difference in the elastic limit is ~ 5%. Concerning failure strain, the increase is 47% meaning that the material shows a great predisposition to ductility. This behavior is related to the higher crystallinity in internal pipe layers.</p>

© 2024 MIM Research Group. All rights reserved.

### 1. Introduction

Copolymerized high-density polyethylene (HDPE) pipes continue to find yet greater relevance fields as technical, durable and economical solutions compared to standard metals. New applications involving plastic pipes need an increased deal of safety, more diligence and reliable protective methods especially in pressurized installations such as oil and gas industries [1,2] and nuclear installations [3,4]. To achieve these goals, durability studies are imperative together with rigorous follow-ups of polyethylene pipes properties in order to guarantee optimal performance levels as required by procedural standards. Accessing the local properties of an extruded and rigid polymer bulk, such as thick pipes or reservoirs, is not an easy task, and in many cases, may require the use of slitting and material removal techniques. For instance, given the sensitivity of HDPE to various external parameters, conventional machining operations by material removal must take place under well-studied and appropriately defined conditions. Several studies have

\*Corresponding author: [kamel.chaoui@univ-annaba.dz](mailto:kamel.chaoui@univ-annaba.dz)

<sup>a</sup> [orcid.org/0009-0002-1961-8305](https://orcid.org/0009-0002-1961-8305); <sup>b</sup> [orcid.org/0000-0002-9349-5967](https://orcid.org/0000-0002-9349-5967); <sup>c</sup> [orcid.org/0000-0001-6532-9462](https://orcid.org/0000-0001-6532-9462);

<sup>d</sup> [orcid.org/0000-0003-1423-3203](https://orcid.org/0000-0003-1423-3203); <sup>e</sup> [orcid.org/0009-0004-4393-2817](https://orcid.org/0009-0004-4393-2817)

DOI: <https://dx.doi.org/10.17515/resm2024.150me0714rs>

Res. Eng. Struct. Mat. Vol. x Iss. x (xxxx) xx-xx

investigated the machinability of semi-crystalline polymers such as HDPE, PP (polypropylene) and PA (polyamide). Published studies involving semicrystalline polymers are much more limited to turning, milling, sawing and drilling processes, but the case of grooving remains, until now, deprived of explicit optimized experimental data [5-11].

In the review authored by Alauddin et al. [5], key manufacturing processes such as orthogonal turning, milling, grinding and drilling for both thermoplastics and thermosets were briefly presented together with comments on optimal machining conditions. Also, important properties of plastic materials in relation to machining such as hardness, strength, heat and chemical effects were reviewed. On the other hand, Kaiser et al. [6] considered a comparative study of machined surfaces in three commercial polymers (Acrylic, uPVC and HDPE) while taking into account hardness, temperature, roughness and chip deformation. As expected, it was observed that better surface finish is obtained at higher cutting speed ( $V_c$ ) combined with low depth of cut ( $a_p$ ). Also, it noted that the surface hardness decreased as the temperature raised up due to the nature of amorphous thermoplastic. At the same time, the average temperature at chip-tool interface and the chip deformation were augmented with  $V_c$  and  $a_p$ . The study established that the surface finish was better for acrylics than uPVC and HDPE. At higher  $V_c$  and  $a_p$ , chip microstructure revealed that numerous crack-like flaws were created, while only fewer cracks were noticed at higher  $V_c$  and lower  $a_p$  [6]. Carr and Feger [7] employed single-point diamond to machine several polymers and they found that material type and its viscoelastic properties play a critical role in determining final surface roughness. As properties dependence on time and temperature is high, changing of parameters such as cutting velocity can alter the cutting mechanism from brittle fracture with rough irregular surfaces to ductile material removal with smooth surfaces. Usually, materials with the ability to deform in a ductile manner, tend to react to external cutting tools by rolling around the edge and for lower molecular weight polymers, cracking occurs well before the ductile regime is attained. On the other side, brittle fracture usually occurs in polymers having high glass transition temperature. They concluded that compressibility and tensile strength have significant effects on the relationship between tool rake angle and resultant workpiece surface roughness [7]. Kiass et al. [8] were the first to investigate the variability of mechanical properties across an HDPE-80 pipe using an original idea based on regular filaments machined by grooving. At that time, no optimization study of the machining conditions was performed. It was found that stress properties are increasing when going from outer diameter towards the inner one while strain properties did not show a clear tendency. The root causes of such behavior were attributed to the inherent stress state and crystallinity distribution across wall thickness as a result of differential cooling during melt extrusion and the subsequent temperature gradients. A linear relationship between filament yielding stress and Young's modulus was presented with supporting data from literature. Kaddeche et al. [9] proposed to search for the minimum required surface roughness which corresponds to the lowest cutting forces using Taguchi and grey relational analysis (GRA) methods when machining HDPE-100 pipes. It was found that the prevalent grey relational grade is best described by a recommended turning regime with  $V_c = 188$  m/min,  $f = 0.14$  mm/rev and  $a_p = 3$  mm. Based on the order of importance, the study established that roughness criteria was mostly controlled by  $a_p$  and  $V_c$  while specific cutting force is dominated by  $f$  and  $a_p$ . Hamlaoui et al. [10] employed RSM and ANOVA to study correlations between machining parameters on one side, and on the other side, HDPE surface roughness and cutting temperature. They concluded that the most influencing regime parameter on surface roughness criteria minimization is also  $f$  (feed rate) as all contributions fell within the interval (96-86%). Conversely, both cutting speed and depth of cut remained the main influencing parameters for the cutting temperature. For high industrial productivity, they proposed to use an optimized regime (119 m/min,

0.12 mm/rev and 0.5 mm) which ensures a limited cutting temperature of  $T^{\circ} \leq 32$  °C, well below the maximum allowed as suggested by standardized practices of PE pipes and reservoirs.

Salles and Gonçalves [11] investigated the influence of both cutting speed and feed rate on surface roughness of UHMWPE under turning operation using hard metallic tools. They concluded that UHMWPE reaction is similar that of aluminum and wood turning. Although, cutting temperature was supposed to show noticeable influence on the surface finish, the cutting speed effect remained low. While many investigations related to plastic materials have concluded that  $V_c$  is the main significant parameter, the situation is somewhat different for UHMWPE as  $f$  was found to be the most sensitive factor in roughness creation. The generated chip was continuous and, according to literature, it indicates the utmost attainable industrial quality. Alternatively, Xiao and Zhang [12] found that the viscous deformation of machined thermoplastics (e.g. HDPE) shows a significant impact cutting forces, surface quality and chip geometry. They concluded that the optimal machining regime should not go beyond a limit which provokes visco-plastic tearing or brittle cracking and ought to take into account molecular mobility, polymer tenacity and glass transition temperature [7].

Recently, Mammeri et al. [13] devoted a study to filament manufacturing from HDPE-100 pipe by an orthogonal turning process. Two chief difficulties were encountered: (i) in-plane filament curvature, and (ii) slightly bowed rectangular filament section. Such technical hitches cannot be completely sidestepped because of the nature of material removal by turning operations. However, it was possible to reduce both of them to technically acceptable minimum levels. Besides optimizing cutting temperature and roughness, it was compulsory to introduce a diligent geometric parameter to account for and monitor filament curvature cutback throughout the evolution of the study. Both filament curvature and unbalanced cross-sectional area reduce the possibilities to prepare satisfactory straight-lined tensile specimens which are anticipated for property assessment across pipe wall. RMS and ANOVA results led to an interesting cutting regime combined with an adequate tool geometry ensuring acceptable filament shape and a cutting temperature below 33 °C. The right cutting edge ( $\kappa_r$ ) and rake ( $\gamma$ ) angles were experimentally established and discussed in the case of tough PE turning [13]. Although several studies related to the machining of different polymers and composites have been published, the fact remains that this literature does not include any specific study to the specific grooving operation and its optimization for such viscoelastic materials. Usually, general recommendations with extended intervals are proposed in some guides but do not fulfill the sought solutions for a rigorous work. Besides cutting parameters ( $V_c$ ,  $a_p$  and  $f$ ), important limitations on temperature and roughness are not provided following an optimization approach.

The main objective of this research is to optimize cutting conditions of uniform and regular filaments by grooving operations from an HDPE gas pipe. The filament should cover the entire pipe thickness, i.e., it includes all (technically possible) layers ranging from the outer surface towards the inner one. Subsequently, a series of specimens, with predetermined dimensions, is subjected to tensile tests to reveal effects of the thermomechanical history induced by extrusion on the various embedded mechanical properties.

## 2. Experimental Methods

### 2.1. Material

As mentioned earlier, the experimental strategy was to prepare polyethylene filaments under specific machining conditions in order to study inherent properties as distributed within the pipe wall. The material was an extruded polyethylene pipe from an HDPE-100

resin according to European (EN 1555-2) and Algerian (NA 7591-2) standards. It was purchased from a local supplier of the CHIALI Co. (Sidi Bel-Abbès, Algeria) in the form of a 12 m section pigmented with carbon black [14]. The pipe standard dimension ratio (SDR) is 17.6 and its outer diameter is 200 mm [13-15]. Tables 1 and 2 summarize some key plastic pipe characteristics, based on approved standards, and regularly provided for product quality assurance.

Table 1. Major physical properties

Property	Method	Value
Density	ISO 1183	0.959 (g/cm <sup>3</sup> )
Fluid Flow Index (190 °C/5.0 kg)	ISO 1133	0.23 (g/10 min.)
Softening Temperature Vicat (VST/B/50 K/h (50 N))	ISO 306	74 (°C)
Crystallinity	ISO 11357-3	65.63 (%)
OIT (210 °C)	EN 728	30 (min.)
Carbon Black Content	ISO 6964	2.25 (%)

Table 2. Key mechanical properties for quality assessment

Property	Method	Value
E (23 °C, V = 1 mm/min.)	ISO 527-1	900 (MPa)
$\sigma_Y$ (23 °C, V = 50 mm/min.)	ISO 527-1	23 (MPa)
Tensile Creep Modulus (1000 h)	ISO 899-1	360 (MPa)
Flexural Creep Modulus (4-Point Method, 2000 h)	DIN 19537-2	330 (MPa)
Notched Charpy Impact (23 °C)	ISO 179	26 (kJ/m <sup>2</sup> )
Shore Hardness (Shore D; 3 sec)	ISO 868	63

## 2.2. Grooving Procedure

Fig. 1 shows the machining system specially developed for grooving operations of PE pipe. For this purpose, it is necessary to find a suitable clamping device so as not to damage the pipe surface by spindle jaws. Therefore, a self-tightening sleeve was manufactured to grasp the HDPE pipe segment with sufficient pressure and allow the grooving operation to take place according to the chosen parameters (Fig. 1).

After equilibrating the mounted pipe segment during rotation, machining must be done progressively given that small cylindricity defects in manufactured plastic pipes are common and are tolerated to a certain standard limit. It is essential to note any continuous chip portion damaged or lost due to cylindricity problems is recorded to be considered when identifying the actual length of the obtained strand at the end of one grooving operation. Each cutting step provides one continuous long chip (i.e., filament) in addition of one pipe ring having a pre-fixed width (between 2 mm and 24 mm) according to the nature of the next mechanical tests. Each cutting condition was carried out several times and only the filaments which meet the requirements set by the experimental protocol were kept. Any filament obtained and presenting defects during machining will be rejected because it ought to represent the entire thickness of the pipe.

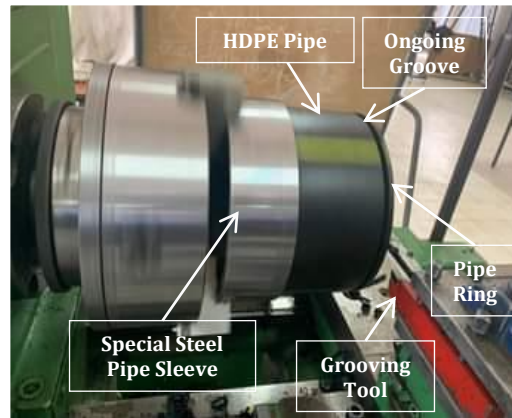


Fig. 1. View of external grooving of an HDPE pipe

Taguchi's planning method was applied for grooving operations in order to organize and carry out the experimental program [10,13,16]. In addition, such optimization is needed to get mathematical models describing the cutting process. Starting with input ( $V_c$ ,  $f$  and  $a_p$ ) and output ( $T$ ,  $R_a$ ,  $R_t$  and filament regularity) factors, the method helped determining the necessary number of tests. Grooving experiments were completed under dry conditions using a SN-40 parallel lathe having 6.6 kW spindle power as explained in literature [9,10,13,15,16]. So as to consider tool geometry, three commercial carbide tools (Type K20) with varying cutting-edge widths were employed. Automatic feeding, in each operation, is given only to the transverse carriage trolley keeping the longitudinal one stationary. The grooving machining conditions allowed to reduce Taguchi L27 plan to L9 while keeping orthogonality and as much as possible output information.

Taking advantage from the method given by Mammeri et al. [13], some choices were straightforward for tool geometry when switching from turning to grooving operations. Ultimately, a  $15^\circ$  positive rake angle ( $\gamma$ ) is defined and both clearance angle ( $\alpha$ ) and cutting-edge inclination angle ( $\lambda$ ) are respectively set equal to  $6^\circ$  and  $0^\circ$ . The cutting-edge angle ( $\kappa_r$ ), which is also called the steering angle, is formed by the cutting edge and the feed direction. It directly affects the cutting length ( $L_c$ ) and resulting chip (or filament) thickness ( $h$ ). The geometrical relationships expressing  $h$  and  $L_c$  as a function of machining conditions ( $f$  and  $a_p$ ) for any angle  $\kappa_r$  are given by equations (1) and (2) [17]:

$$h = f \cdot \sin(\kappa_r) \quad (1)$$

$$L_c = \frac{a_p}{\sin(\kappa_r)} \quad (2)$$

Since grooving operations on HDPE pipe are characterized by a  $90^\circ$  cutting-edge angle ( $\kappa_r$ ); therefore,  $L_c$  and  $h$  are respectively identified as depth of cut ( $a_p$ ; mm) and feed rate ( $f$ ; mm/rev). Consequently, filament regularity was easily checked as no out-of-plane bending or deviation ought to occur; i.e., curvature is obviously nil. This situation is sought by such experimental program for subsequent uniaxial filament testing. It should be noted that commercial HDPE pipes are not perfectly circular at outer and inner surfaces. Thus, complete grooving of a continuous filament took place after some initial pipe revolutions to correct cylindricity along its z-axis.

### 2.3. Roughness and Temperature Measurements

Roughness measurements were carried out in the longitudinal direction of the filament's outer side using a MITUTOYO SurfTest 301M roughness meter as explained elsewhere for turning and grooving [13,15]. Two roughness criteria (i.e., Ra and Rt) were chosen in order to have a comprehensive understanding of the readily accessible filament surface. This choice is kept alike for all experiments with 3 different measurements.

Filament surface temperature was measured as close as possible to the cutting zone. Its determination was achieved during the machining operations with a CAT-S60 smartphone equipped with a Lepton 2.5 sensor for the FLIR (Forward Looking InfraRed) thermal camera (Fig. 2). With an accuracy of  $\pm 2.0$  °C, it allows temperature measurements in the range of -20 to 120 °C with a good thermal sensitivity well-adapted to moving parts and black objects [13,18].



Fig. 2. Temperature measurement set-up using CAT S60 smartphone [13]

A special support was engineered to fix the camera with the possibility of orienting it according to the demand. The support consists of two mechanisms: the first one allows to hold firmly the smartphone to the upper tool holder trolley via a switching magnet and the second one is an articulated support commanding camera movement in three directions. Preliminary tests were carried out to delimit the measurement zone and the principal thermal scene parameters (i.e., emissivity, remoteness, atmospheric temperature, reflection, measurement angle and color palette). For each test, at least three measurements were taken during machining stabilization period towards the end of the operation.

### 2.4. Stress-Strain Tests

Mechanical In the second part of this work, variances of mechanical properties across pipe wall were investigated using monotonic tensile tests of filament specimens based on the general recommendations of ISO 527 standard. The stress-strain curves ( $\sigma$ - $\epsilon$ ) are obtained on a universal Zwick/Roell testing machine Type BT 1-FR2.5TN.D14. Its load cell type is a KAP-TC with a force limit of 2 kN. The operating system and data acquisition are controlled by the TestXpert® 2.0 Software, as indicated in Fig. 3.

Finite specimens were cut from the original long filament extending from outer pipe surface all-the-way through the wall. Each specimen is associated with a unique numeral, checked for any damage, then calibrated and the necessary observations are documented.

As a whole, the obtained filament is accepted as a wide-ranging representation of juxtaposed material layers forming the pipe wall thickness.

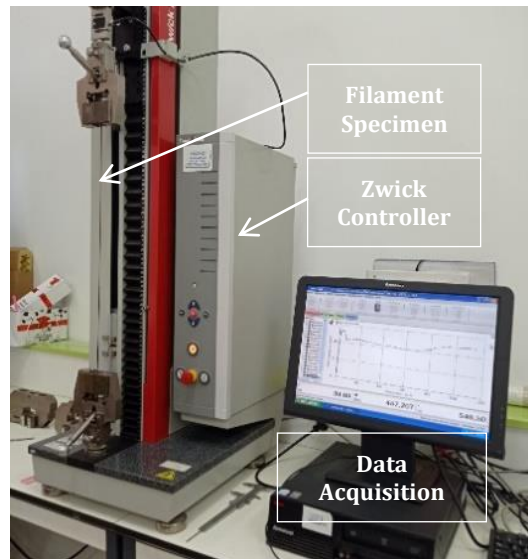


Fig. 3. Zwick universal tensile testing machine and TestXpert data acquisition system

The numbered layers can be assumed as a series of circumscribed rings with decreasing diameters from the outer side towards the inner side of the pipe. From each layer, an ordered succession of specimens of finite size ( $120 \times 4 \times 0.4 \text{ mm}^3$ ) was prepared and the remaining piece whose length is below 120 mm were saved for other purposes. The stress-strain curves ( $\sigma$ - $\epsilon$ ) are obtained at 50 mm/min.

### 3. Results and Discussion

#### 3.1. Filament Assessment

Fig. 4 shows the resulting machined filament by grooving as it starts at the outer pipe surface (Yellow mark) and it ends at the inner side (Deformed end). Throughout the machining operation, the cutting process is closely monitored to guarantee steadiness and continuousness of the removed material (i.e., the filament). The latter is considered as a manufactured product known conditions (cutting regime, cutting temperature, tool geometry, and at a given position along the pipe length) and hence, can be used for characterization (mechanical, structural, etc.). Each obtained filament is carefully spool-lose and stored in a plastic bag with an appropriate identification to avoid any alteration or damage.

In this study, the conditions for machining and tool selection have been improved compared to previous studies [8-10,16], making it possible to get even smaller filament thicknesses. However, these improvements unveiled the limits of quality parameters of marketed HDPE pipes especially for out-of-roundness and thickness tolerances. In fact, if the pipe is not accurately cylindrical, dimensional approximations must be made to reach thresholds which helps identifying the positional coordinates (radial and circumferential) of the specimen for each 0.4 mm thick layer. In other words, it is sometimes tolerated to lose a few layers, at the machining start-up, until the cutting process becomes unfluctuating and the produced filament is continuous and regular. Therefore, it is

necessary to consider these inevitable difficulties, since rectifications altering the pipe stress state or the polymer structure are not tolerated herein.

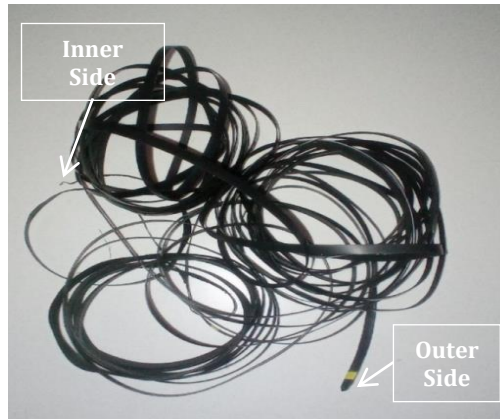


Fig. 4. A overall filament manufactured by grooving

The same approach is also effective for some layers at the innermost side which might be lost due to excessive deformations and material distortions. In all cases, it is necessary to take these adverse events into account during each cut. In addition, it is advised to make the appropriate choices to reduce the width and the mass of the resulting ring associated with each prepared filament.

### 3.2 Machining Optimization

#### 3.2.1 Taguchi Orthogonal Plan

The three cutting parameters levels are chosen based on published data, guidelines for plastics machining and on specific previous studies for similar polycrystalline polymers [8-11,19-21]. Following a previous study on turning of HDPE pipe material [13,15], lower and upper limits for  $V_c$ ,  $f$  and  $a_p$  are respectively (100 – 560 m/min), (0.34 – 0.63 mm/rev) and (2 – 3 mm) whereas, the intermediate levels are 140 m/min, 0.49 mm/rev and 4 mm as indicated in Table 3.

Table 3. Selected levels for cutting parameters

Level	$V_c$	$f$	$a_p$
	(m/min)	(mm/rev)	(mm)
1	100	0.34	2
2	140	0.49	3
3	560	0.63	4

Conventional cutting factors ( $V_c$ ,  $f$  and  $a_p$ ) are considered as input parameters while performance characteristics comprise ( $T$ ,  $R_a$ ,  $R_t$  and  $L$ ). The geometrical parameter  $L$ (mm), defined in [13] as a gap representing a specified deviation between bent and straight filaments observed in the case of turning. Output parameters are recorded during or after the grooving operation depending on the case using a simplified Taguchi L9 mixed level (Table 4). In grooving operations, the parameter  $L$  representing the height of filament bent is visually and physically checked against a metallic straight ruler. As expected for grooving and the for the selected tool geometry, it is nil all the times (i.e., no curvature) and this is a reliable corroboration for the filament uniformness and levelness. It is observed that high  $V_c$  (560m/min) for all  $f$  levels (0.49; 0.63 and 0.34 mm/rev) produced unacceptable cutting

temperatures which exceeded or nearly equated the 40°C limit; thus, level 3 cannot lead to desirable machining regime regardless of  $a_p$  values.

Table 4. L9 Taguchi experimental plan for HDPE grooving operations

Run N°	Cutting Parameters			Performance Characteristics			
	Vc (m/min)	f (mm/rev)	$a_p$ (mm)	T (°C)	Ra ( $\mu\text{m}$ )	Rt ( $\mu\text{m}$ )	L (mm)
1	100	0.34	2	32.9	0.44	0.97	0
2	100	0.49	3	35.3	0.45	1.05	0
3	100	0.63	4	36.2	0.49	1.13	0
4	140	0.34	4	35.9	0.20	0.82	0
5	140	0.49	2	34.1	0.29	0.88	0
6	140	0.63	3	34.8	0.31	0.97	0
7	560	0.34	3	39.4	0.29	0.75	0
8	560	0.49	4	44.3	0.23	0.86	0
9	560	0.63	2	43.5	0.30	0.93	0

It is understood that heat generation is intensely triggered when polymers are subjected to rapid frictional material removal operations. The lowest roughness value (Ra: 0.20  $\mu\text{m}$ ) is recorded at 140 m/min and 0.34 mm/rev which corresponds to an acceptable measured T (35.9 °C). From literature of polymer machining, it is known that lowering Vc, f and  $a_p$  can lower the generated heat but, usually it follows that roughness criteria are catastrophically degraded [13,19,20].

### 3.2.2 ANOVA Approach

ANOVA conclusions on how initial regime factors affected the selected output parameters (Ra, Rt and T) are depicted in the following Tables 5–7. In all cases, Vc can be considered as the most significant factor among the regime parameters while  $a_p$  is the less affecting factor.

Table 5. ANOVA of Ra

Source	DF	Seq SS	Contribution	Adj SS	Adj MS	F-Value	P-Value
Model	5	0.082779	99.26%	0.082779	0.016556	79.97	0.002
Linear	3	0.027935	33.49%	0.059173	0.019724	95.27	0.002
Vc	1	0.021162	25.37%	0.051872	0.051872	250.55	0.001
f	1	0.004756	5.70%	0.002144	0.002144	10.35	0.049
$a_p$	1	0.002017	2.42%	0.004245	0.004245	20.50	0.020
Square	1	0.051105	61.28%	0.051105	0.051105	246.84	0.001
Vc*Vc	1	0.051105	61.28%	0.051105	0.051105	246.84	0.001
2-Way Interaction	1	0.003739	4.48%	0.003739	0.003739	18.06	0.024
Vc*f	1	0.003739	4.48%	0.003739	0.003739	18.06	0.024
Error	3	0.000621	0.74%	0.000621	0.000207		
Total	8	0.083400	100.00%				

Table 6. ANOVA of Rt

Source	DF	Seq SS	Contribution	Adj SS	Adj MS	F-Value	P-Value
Model	5	0.100591	99.77%	0.100591	0.020118	260.62	0.000
Linear	3	0.073017	72.42%	0.096247	0.032082	415.60	0.000
Vc	1	0.039764	39.44%	0.062300	0.062300	807.06	0.000
f	1	0.032187	31.92%	0.033796	0.033796	437.80	0.000
ap	1	0.001067	1.06%	0.002191	0.002191	28.38	0.013
Square	1	0.025725	25.52%	0.025725	0.025725	333.25	0.000
Vc*Vc	1	0.025725	25.52%	0.025725	0.025725	333.25	0.000
2-Way Interaction	1	0.001849	1.83%	0.001849	0.001849	23.95	0.016
Vc*f	1	0.001849	1.83%	0.001849	0.001849	23.95	0.016
Error	3	0.000232	0.23%	0.000232	0.000077		
Total	8	0.100822	100.00%				

For Ra, cutting speed contribution is in the lead with Vc and Vc<sup>2</sup> (respectively 25.37% and 61.28%). Similarly, for Rt, both forms of speed (Vc and Vc<sup>2</sup>) dominate with respective contributions of 39.44% and 25.52%. When it comes to cutting temperature which is supposed as the main limiting parameter in this process, the effect of Vc is much more pronounced since it explains 83.87% of total differences. It is noted that the contributions of ap in both cases did not exceed 3%. 7).

Table 7. ANOVA of T

Source	DF	Seq SS	Contribution	Adj SS	Adj MS	F-Value	P-Value
Model	4	133.142	98.76%	133.142	33.285	79.54	0.000
Linear	3	125.603	93.17%	132.310	44.103	105.40	0.000
Vc	1	113.075	83.87%	112.159	112.159	268.04	0.000
f	1	6.726	4.99%	11.049	11.049	26.40	0.007
ap	1	5.802	4.30%	10.803	10.803	25.82	0.007
2-Way Interaction	1	7.538	5.59%	7.538	7.538	18.02	0.013
Vc*f	1	7.538	5.59%	7.538	7.538	18.02	0.013
Error	4	1.674	1.24%	1.674	0.418		
Total	8	134.816	100.00%				

The feed rate contribution is important for Rt as the latter represents the height change between the topmost and the deepest points within a given measuring section while Ra is just an average variation of the roughness profile from a reference line. The averaging operation leads to lower Ra than actual roughness variations and keeps them always well below corresponding Rt measurements. For cutting temperature, it is concluded that Vc is dominant with more than 83% contribution (Table

Alternatively, Fig. 5 represents the variation of the responses in terms of Ra, Rt and T as a function of the most influencing input parameters (f and Vc) as deduced from the ANOVA section. As anticipated, both Ra and Rt describe a comparable shape represented by a steep decrease up to ~300 m/min followed by a sharp rise at higher speeds (Figs. 5a-5b). It appears that 300 m/min is a critical point which indicates the lowest values of Ra and Rt especially when feed rate f is at its minimum.

The effect of f on roughness criteria remains small within the range shown (0.30-0.66 mm/rev) and at low cutting speeds, the corresponding variations ( $\Delta Ra$ ) and ( $\Delta Rt$ ) are respectively  $\sim 0.2 \mu\text{m}$  and  $\sim 0.5 \mu\text{m}$ . In both cases, the global roughness values are lowermost for speeds in the range 250-350 m/min. However, when invoking temperature as a limiting criterion for material integrity, it is observed that at higher speeds ( $V_c > 300$  m/min), generated heat becomes a detrimental factor and lead to material degradation (Fig. 5c) especially at higher feed rates.

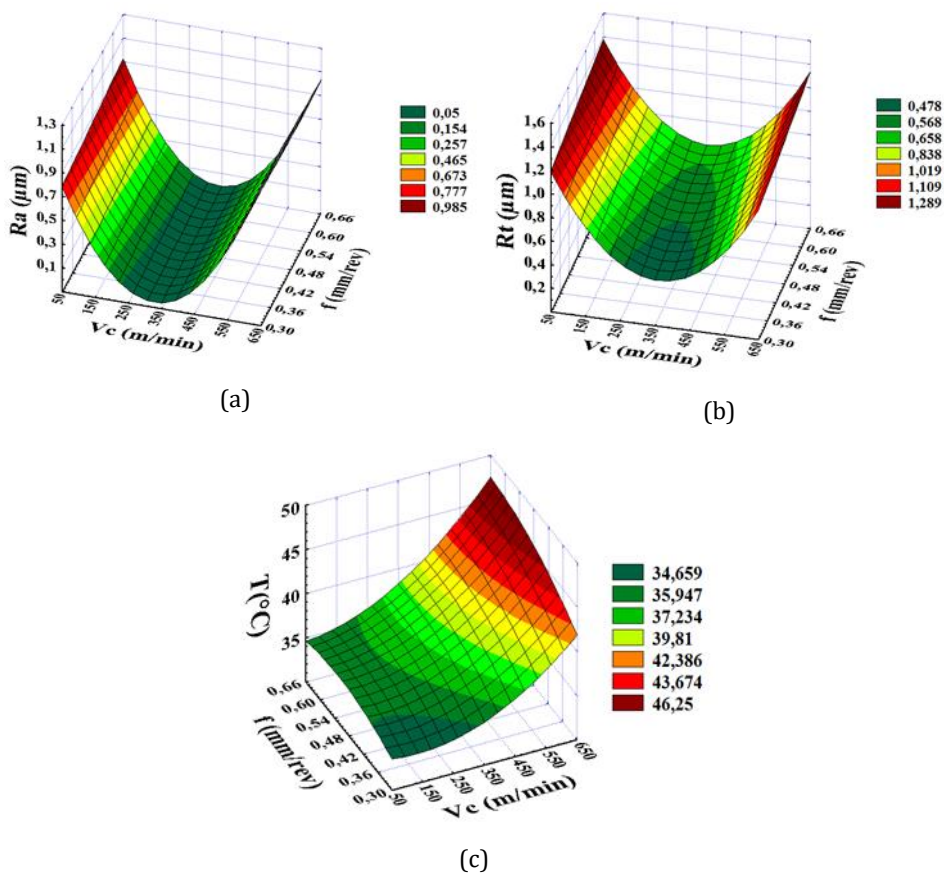


Fig. 5. Estimated response surface of performance characteristics versus  $V_c$  and  $f$

### 3.2.3 Grooving Conditions Optimization

The optimization results are presented Table 8. The case evoking no constraints on both roughness criteria and cutting temperature is chosen. The reason is that only one most significant input factor (i.e.,  $V_c$ ) is found and there is a high probability that the associated

limiting temperature is well below the maximum set by the standards as shown from the experimental results.

Table 8. Parameters (8a) and optimization (8b) solution

	Response Parameters	Goal	Lower	Target	Upper	Weight	Importance
(8a)	Rt	Target	0.95	1.10	1.33	1	1
	T	Target	32.90	36.50	44.30	1	1
	Ra	Target	0.20	0.22	0.49	1	1

(8b)	Vc (m/min)	f (mm/tr)	ap (mm)	T (°)	Ra (µm)	Rt (µm)	Composite Desirability
	137.194	0.4	4	36.448	0.223	1.100	0.991034

The targeted performance values with identical weights and importance levels together with the optimized parameters are shown in Tables 8a and 8b. When using the optimal desirability, the anticipated practical solution for grooving consists principally of a moderate cutting speed (137 m/min) and an acceptable cutting temperature (36.5 °C). HDPE literature does not report temperature data for grooving but for turning there is some similarities [9,10,13,16]. It is concluded that this optimization gives satisfactory parameters for the sought application under grooving process and the filaments can be employed to investigate property variances across the pipe wall. Fig. 6 indicates the response optimization for T, Ra and Rt.

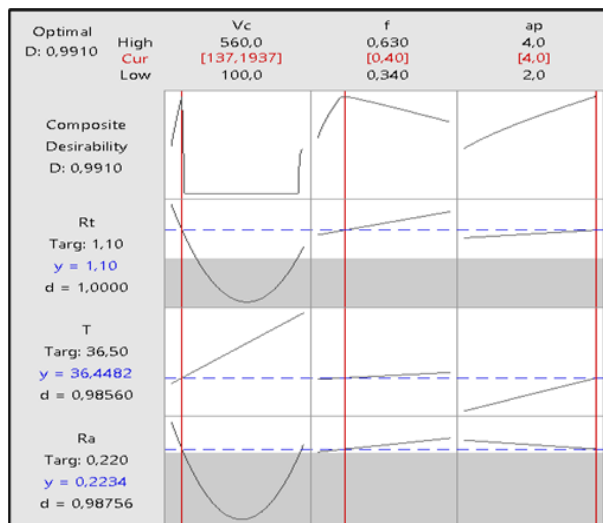


Fig. 6. Response optimization for T, Ra and Rt

Again, it is revealed that Vc is the most influencing factor for grooving process and its important effects on T are evident. On the other hand, both f and ap show limited effects on output parameters. As discussed in literature, PE is subject to heat induced phenomenon which may ultimately cause irreversible damage [11,12].

At this stage, it is interesting to discuss the corresponding regression equations which include all parameters and their interactions. It is understood that the models are reduced by eliminating terms with no significant effects on the responses. The final models of response equations in terms of input factors are as follows:

$$R_a = 0.9665 - 6.926 \cdot 10^{-3} V_c + 0.4336 f - 0.02887 a_p + 1.1 \cdot 10^{-5} V_c^2 - 8.98 \cdot 10^{-4} V_c \cdot f \tag{3}$$

$$R_t = 1.4870 - 5.686 \cdot 10^{-3} V_c + 0.3366 f + 0.02074 a_p + 7.0 \cdot 10^{-6} V_c^2 + 6.31 \cdot 10^{-4} V_c \cdot f \tag{4}$$

$$T = 30.15 - 2.59 \cdot 10^{-3} V_c - 3.45 f + 1.456 a_p + 0.04032 V_c \cdot f \tag{5}$$

In order to appreciate the goodness-of-fit, calculated R<sup>2</sup>, adjusted R<sup>2</sup> and standard error of the estimate are summarized in Table 9. It is observed that the coefficients R<sup>2</sup> (i.e., the percentage of the variation in the response that is explained by the model) and R<sup>2</sup> adjusted (i.e., which represents R<sup>2</sup> when adjusted for the number of predictors in the model relative to the number of experimental observations; filament roughness criteria and temperature) are very satisfactory for all output model parameters. The standard errors of the regression (or standard errors of the estimate) indicated by (S) are also very satisfactory compared to the experimentally measured data.

Table 9. R<sup>2</sup>, R<sup>2</sup> adj. and s for output parameters

Output model parameter	R <sup>2</sup> (%)	R <sup>2</sup> Adjusted (%)	S
T	98.76%	97.52%	0.6468 °C
Ra	99.26%	98.01	0.01438 μm
Rt	99.77%	99.39	0.00878 μm

It is accepted that common deviation sources between actually measured and statistically estimated data are diverse and they can be imputed to many circumstances proper to this study: (i) each experimental value used in the modeling is the result of an average value issued from 3 distinctive and consecutive measurements for the same test; (ii) in fact, the obtained statistical models are just approximation models and not interpolation functions; (iii) both uncertainties and engendered errors accumulated during testing may be in relation with the machine-tool condition, the chosen measuring instruments (roughness and temperature), the operator etc.; and finally, (iv) residual errors created when carrying out ANOVA analysis following the hypothesis of 95% confidence interval.

The following Table 10 illustrates cutting regime parameters adopted in different studies devoted to polyethylene machining and typical limits for various outputs. It is observed that both feed rates and depths of cut are well positioned in specific intervals dictated by polymer thermal and structural properties which are a basis for the corresponding industrial standards. However, cutting speed is variable over a wide range as it greatly influences production objectives (material removal rate) and product quality. It is found that the majority of optimization studies indicate Vc < 200 m/min. limit. In comparison to turning, reducing Vc for the grooving process contributes to obtain acceptable properties for the machined filaments.

Table 10. Comparison of literature data for PE martials machining

machining process	Cutting parameters			Output parameters		Refs
	f (tr/min.)	ap (mm)	Vc (m/min)	T (°C)	Ra (µm)	
Turning	Constant (0.254)	0.5-4	3-27.5	33-45	3.5-6.8	[6]
Grooving, HDPE-80	0.5	2	17.66	Variability of ( $\sigma$ - $\epsilon$ ) behavior across pipe wall		[8]
Turning, HDPE-100	0.14	3	188	<40	2.25	[9]
Turning, HDPE-100	0.12	0.5	119	32	0.86	[10]
Turning, UHMWPE	0.025-0.3	Constant (~0.4)	160 - 400	Max. advisable service T°: 93°C	1.5-9	[11] *
Turning, HDPE	0.01	1.47	50	Lowest surface roughness		[21]
		1	150	Highest material removal		
		1.5	100	Largest chip thickness		
Turning, HDPE-100	0.37-0.67	2-4	100-560	28.5-39.5	0.41-1.55	[13]
	0.5	4	160	32	0.46	
Grooving, HDPE-100	0.34-0.63	2-4	100-560	32.5-44.3	0.20-0.49	**This study
	0.4	4	137	36	0.223	

\*: Min. Mw = 3.1x10<sup>6</sup> g/mol.; Chip formation study; \*\*: based on optimized regime parameters of [13].

### 3.3 Mechanical Properties Crosswise Pipe Wall

In this second part, the outlines of a practical validation are considered in order to complete the procedure of manufacturing and testing filament specimens. At this stage, the primary objective was to obtain stress-strain behaviors and analyze few specific mechanical properties to get a first sense of the tendencies across the wall pipe.

#### 3.3.1 Assorting Test Specimens

The matching process for specimens made out of the overall filament is summarized in Fig. 7. Indeed, just after machining and recording the production parameters, the global filaments (chip) can be viewed in “rolled-up” (Fig. 7a) or “scrambled” (Fig. 7b) forms which are influenced by relieved internal stresses [21-23]. The latter is not particularly preferred as it increases the probability of filament entanglements and unwanted deformations during handling and storage. After identification of the yellow marks (external surface), dimensional measurements and examination of the 2 filament tips, the positions of the layers are identified and finally separated from each other (Fig. 7c). As the cumulative set of layers represents the pipe wall thickness; then, the length of one given layer is equivalent to the pipe diameter at that radial specified position.

It is necessary to record the sequential order of each 120 mm long segment as it appears and in a clockwise direction to obtain the number of specimens per layer of material. For instance, in Figs. 7c-d, the operation provided 4 effective specimens and one residue (i.e.; specimen length < 120 mm). This operation is repeated for the next layer until all layers are completed.

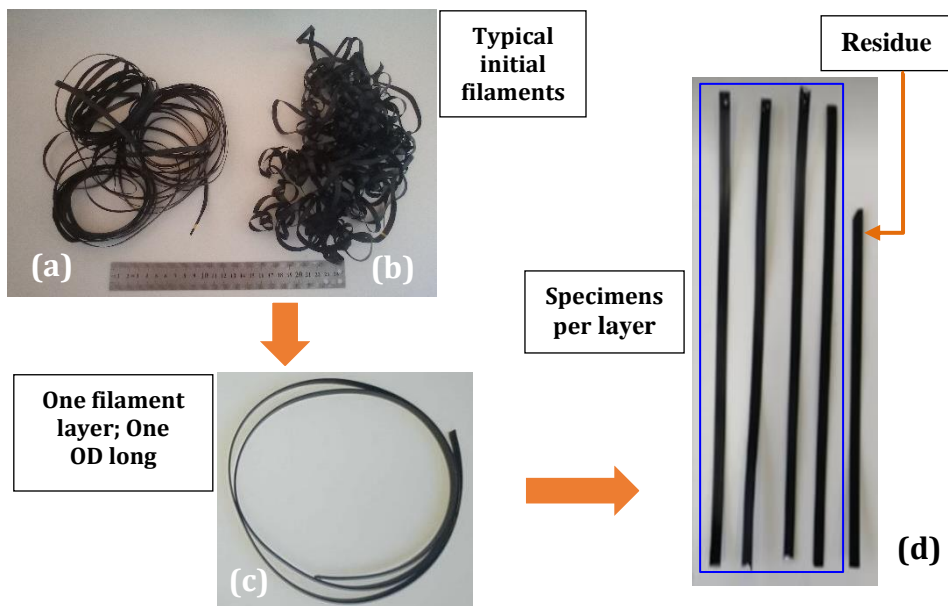


Fig. 7. Steps for testing specimen cutting

### 3.3.2 Tensile Characterization

Specimens subjected to monotonic traction show similar stretching behavior characterized by single or multiple necking zones as illustrated in Fig. 8. Initiation locations of drawn-out zones propagation direction remain aleatory. In some cases, one drawn zone begins around the specimen's mid-span and at the same time, starts propagating towards both grips (Fig. 8a). In other cases, the opposite occurs and the necking begins on the side of the jaws and evolves towards the middle of the specimen, forming one or multiple "spindles" of unstretched material (Fig. 8b).

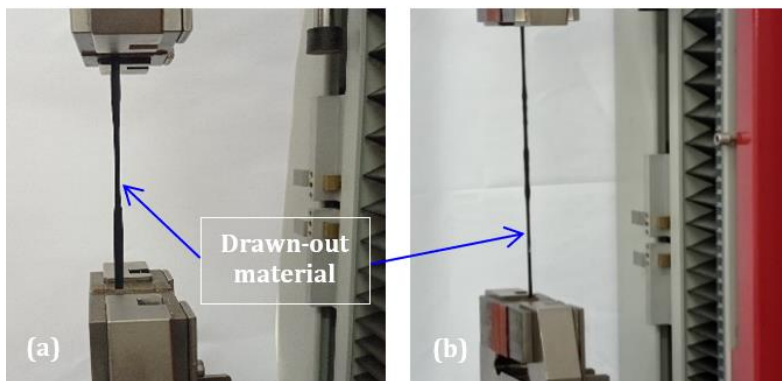
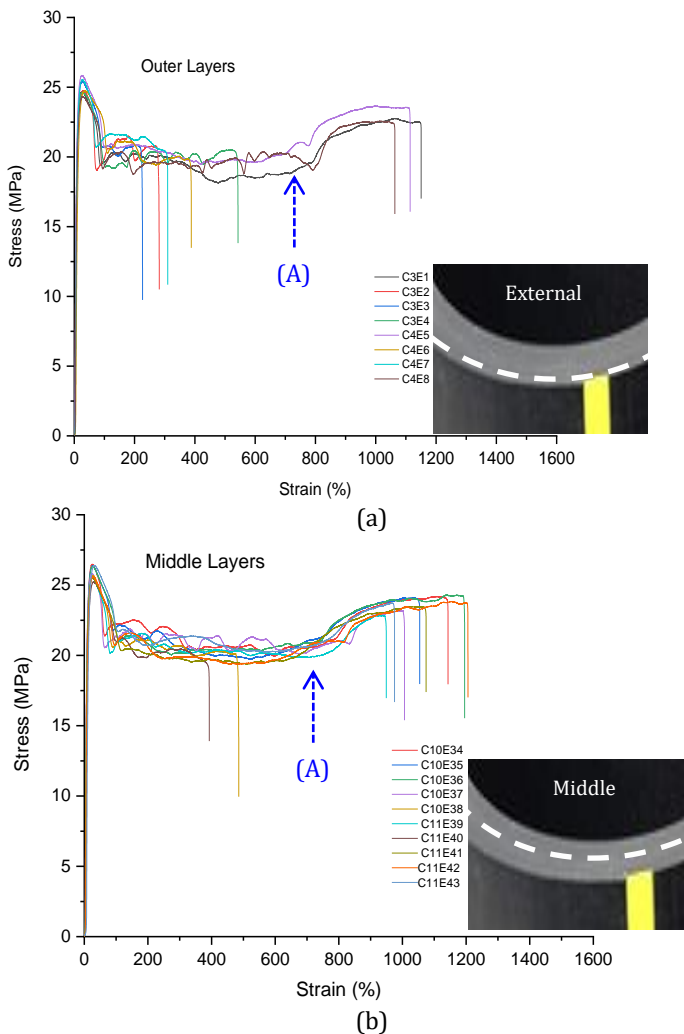


Fig. 8. Photographs of filament behavior under monotonic traction

In Fig. 9, a series of 25 tensile tests, carried out in the same laboratory conditions, is shown. They portray 3 different batches of successive layers located at average diameters of 196 mm, 188.6 mm and 179.2 mm respectively for outermost (Fig. 9a), intermediate (Fig. 9b) and innermost (Fig. 9c) layers. Each batch can be regarded as a cylindrical envelope with a total thickness  $\leq 4$  mm. In all cases, stress-strain ( $\sigma$ - $\epsilon$ ) curves replicate global similarities including a relatively narrow elastic zone and a widened plastically drawn zone as it is typically observed for semi-crystalline polymers. Physically, the last zone associates a cold drawing part which occurs at relatively constant stress and a final phase including plastic hardening and a tremendous rise in polymer chain orientation.

This behavior has already been observed in the literature for HDPE filaments and standard specimens in virgin and chemically aged conditions from engineering stress-strain curves [8,23-28]. Comparing behaviors of outer and inner layers (Figs. 9a, 9c), it is observed that the measured deformations at break increased significantly (from  $\sim 1100\%$  up to  $\sim 1500\%$ ) and the elastic resistance is also gradually increasing (from  $\sim 25$  MPa up to  $\sim 28$  MPa). On the other hand, the cold drawing part (middle zone) has rather shrunk in favor of increased plastic hardening and chain orientation [12,29-32].



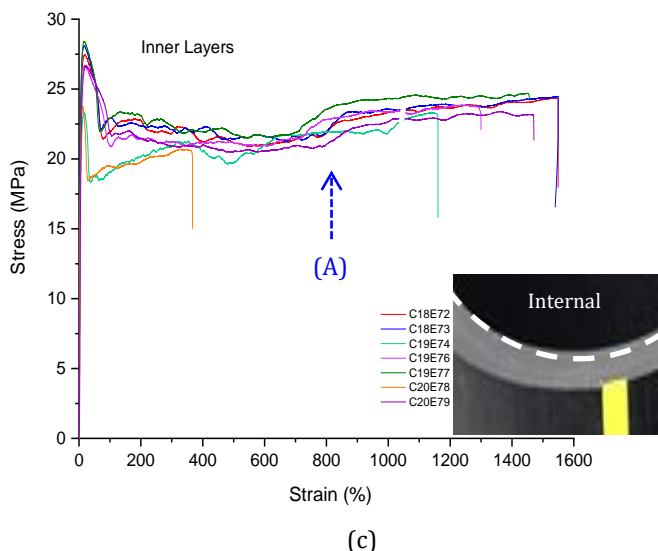


Fig. 9. Stress-Strain curves: (a) outer, (b) middle and (c) inner pipe layers

This suggests that the inner layers are much stronger than the outer layers. Undoubtedly, the pipe extrusion process is at the origin of these variations which were possible to reveal via such experimental methodology. Indeed, the abrupt cooling by intense water showers allows stored heat to be evacuated from the bulky mass of polyethylene while it is in the solidification phase. Also, this action does not allow material stress relaxation in a uniform manner, i.e., the internal layers remain sufficiently hot and experience slow cooling by natural convection as opposed to the external layers. These conditions favor embedding residual (internal) stresses and morphology variances in the pipe structure in terms of crystalline and amorphous parts [21-24,29-32].

### 3.3.3 Mechanical Properties Variability

The quantitative analysis of  $\sigma$ - $\epsilon$  curves makes it possible to extract several mechanical properties relating to resistance, elasticity and ductility. Table 11 shows the values of Young's modulus, elastic limit, yield strain and strain at break as a function of position in the pipe wall. In this case, 3 distinctive locations in the pipe wall are chosen with corresponding layer samples to elucidate differences. The values shown in Table 11 are averages of several tests for each layer as deduced from Fig. 9. Analyzing these results across the pipe wall (i.e., from outermost to innermost envelope), it appears that tendencies are manifested by an increase in  $E$ ,  $\sigma_y$  and  $\epsilon_f$  while  $\epsilon_y$  is showing a manifest decline. When switching from one layer to the next one, it is possible to perceive the variation (or the progression) of illustrated properties from one layer to another within one given envelope. At this level, it is noted that this progression does not follow only one trend, as the averages of most measured values for the innermost envelope are effectively fluctuating. Also, the greatest dispersion of results is found for the strain at failure, which is predictable because of the large stretching values especially for the layers located on the pipe internal side. Usually, the structure is supposed to be much more crystalline and what remains from the positive residual stresses is added to the applied load.

Fig. 10 depicts averaged properties for each of the 3 envelopes (outermost, midway and innermost). It is found that pronounced trends characterize these properties along the pipe radial direction. For both  $E$  and  $\sigma_y$ , the innermost layers are found to be more rigid and more resistant (Figs. 10a-b). These findings corroborate with the structural properties such as the degree of crystallinity and the morphology (e.g., lamellae thickness, tie-

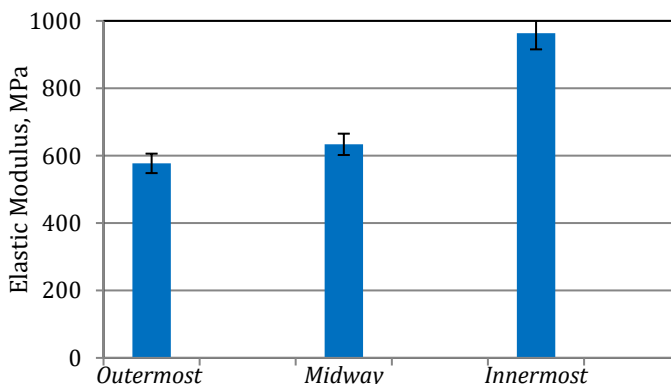
molecules density, etc.). On the other hand, as shown in Figs. 10c-d, the properties related to yield and failure strains are in opposite evolutions. The highest property variation between outermost and innermost envelopes is recorded for  $\epsilon_f$  with +51.3% followed respectively by E (+40.1%),  $\epsilon_y$  (-39,5%) and  $\sigma_y$  (+10.3%).

Table. 11. Mechanical properties of HDPE tube through the wall

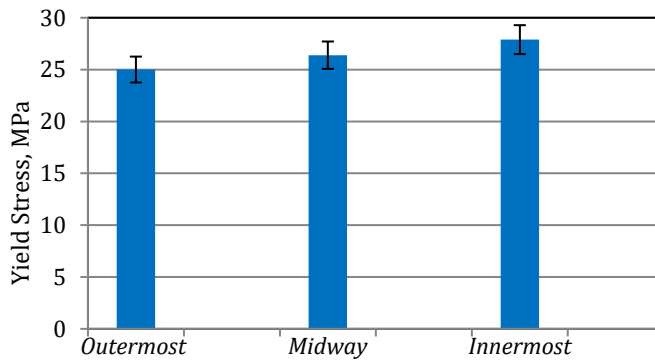
Position in Pipe Wall	Layer Nb	Nb of specimens*	E (MPa)	$\sigma_y$ (MPa)	$\epsilon_y$ (%)	$\epsilon_f$ (%)
Outermost	3	(4)	573.75 (±38.75)	24.86 (±28)	27.03 (±1.26)	560.69 (±30.75)
	4	(4)	580.60 (±31.75)	25.15 (±0.49)	27.35 (±1.14)	801.40 (±24.46)
Midway	10	(5)	651.20 (±38.64)	26.42 (±0.18)	25.87 (±1.04)	1113.65 (±83.35)
	11	(5)	616.17 (±8.75)	26.36 (±0.29)	26.36 (±0.29)	1050.38 (±88.87)
Innermost	18	(2)	1005.99 (±1.11)	28.45 (±0.015)	16.37 (±0.37)	1500** (-)
	19	(3)	923.25 (±86.22)	28.19 (±0.30)	16.24 (±0.38)	1327.61 (±101.14)
	20	(2)	961.89 (±38.00)	27.05 (±0.95)	16.75 (±0.25)	1467.95 (±543.97)

\* Valid; \*\*Maximum machine crosshead displacement reached.

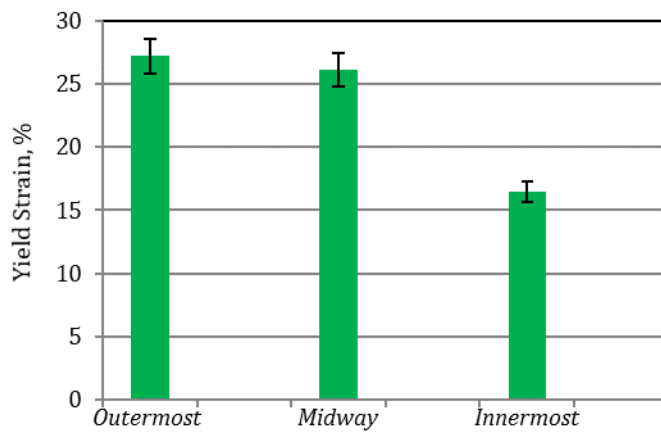
Furthermore, when the pipe wall thickness is conceived as 2 concentric envelopes: (i) an external one extending from outer-to-middle and, (ii) an internal envelope laying from middle-to-inner, the observed variations are quite different. Fig. 10 shows that the inner envelope (midway–innermost) presents the dominating variations for both E (+34.2%) and  $\epsilon_y$  (-37.0%). Inversely, the highest variation for  $\epsilon_f$  is associated with the outer envelope (outermost–midway) with 37.1%. In the case of yield stress, there is an equivalent contribution for both sides with roughly 5%. Although it is not easy to explain what happens during a traction test from the macromolecular point of view but polymer characterization techniques helped to disclose some understandings in the course of the last thirty years [31,32]. Some foremost conclusions on tensile behavior of polyethylene are reviewed in the following paragraphs.



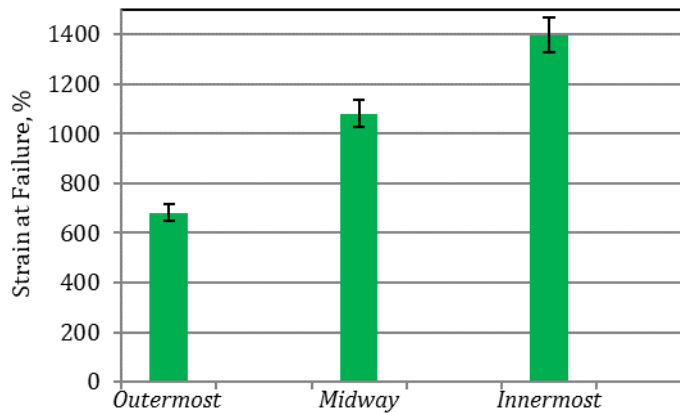
(a)



(b)



(c)



(d)

Fig. 10. Evolution of (a)  $E$ , (b)  $\sigma_y$ , (c)  $\epsilon_y$  and (d)  $\epsilon_f$  as a function in pipe wall

Using X-ray diffraction, Addiego et al. [31] concluded that monotonic traction of HDPE is associated with a significant volume change caused by local polymer chain

transformations affecting the semi-crystalline structure. The strained structure shows a progressive crazing mechanism at the spherulitic level followed by a cavitation phenomenon and subsequently, intense fibrillation restricting conventional chain movements. They also explained that a rivalry opposes volume increase and chain compaction respectively generated by crystallinity diminution (narrowing of the ordered domain) and chain orientation especially occurring throughout drawing and strain hardening phases. It is understood that both homogenous and inhomogeneous processes characterize the HDPE structure. In the first mechanism, the spherulites' dilatation is global (multidirectional) while for the following one, subsequent yielding occurs unevenly favoring the formation of crazes [30-32].

At another level, the interlamellar connections known as tie-molecules usually work as draw back momentum towards the original material state upon unloading. They contribute in conveying present loads from extended amorphous regions towards crystalline ones which undergo plastic deformation [32,33]. Séguéla [33] concludes that stress concentration on infinitesimal structural weaknesses lead to unexpected crazing mechanism which develops slow crack growth (SCG). Also, fragmented lamellae and unfolded polymer chains contribute to the fibrillar structure which constitutes drawn material which prolongs from the strain at yield location up to the onset of plastic strain hardening designated by arrow (A) in Fig. 9. This is one good reason to prefer the copolymerization process for HDPE as it favors the increase of intercrystallite tie-molecules and hence, ameliorates the long-term pipe resistance. According to an in-situ investigation carried out on the strain hardening occurrence in PE, it was confirmed that it is the result of the highly stretched tie-molecules fraction bonding the well-ordered chains [34].

## 5. Conclusion

Although a lot of research studies on plastics and composites machining are available, very few of them investigated the grooving process of semicrystalline polymers. The practicality of this work lies in the manufacture of filament specimens to retrace the thermomechanical history of an extruded pipe from copolymerized HDPE resins. The following conclusions may be drawn:

- Based of RSM, this study investigated the optimization of grooving regime to manufacture continuous polyethylene filaments from HDPE-100 gas pipe. The grooving operation is initiated from outer to inner pipe surface.
- In order to preserve the filament integrity, more attention is paid to cutting temperature as a key limiting parameter in this process. The effect of  $V_c$  is more pronounced as it explained 83.87% of total differences while the contribution of  $a_p$  did not exceed the 5% threshold. As expected,  $R_a$  and  $R_t$  described a comparable behavior illustrated by one "decrease-increase" sequence with a minimum around 300 m/min. It appears the 300 m/min cutting speed is an interesting point when searching for the lowest  $R_a$  and  $R_t$  values for a minimum feed rate. However, when considering cutting temperature, it is found that as  $V_c$  goes beyond this limit ( $V_c > 300$  m/min), more heat is generated and becomes a detrimental factor for material integrity especially at greater feed rates.
- The optimized solution (for a desirability  $\sim 1$ ) is characterized by very satisfactory roughness criteria and cutting temperature. The latter is well below the 40 °C imposed by HDPE pipes standards. A cutting speed of 137 m/min is also acceptable as the process of filament grooving should be carried out meticulously in order to increase reliability of afterward measured mechanical and/or structural properties.

- In all tested cases, the stress-strain curves as a function of 3 radial pipe wall locations duplicated overall similarities comprising a narrow elastic zone and a widened plastic one (drawing and hardening phases) typically observed for semi-crystalline polymers. However, they revealed interesting variances in terms of mechanical properties which are in phase with structural explanations given in literature.
- Young's modulus, yield stress and strain at break increased from outermost to innermost layers which suggests that pipe inner layers are much more stiff, resistant and show significant ductility. Across the pipe wall, the increases of  $E$ ,  $\sigma_y$  and  $\epsilon_f$  are respectively +40.1%, +10.3% and +51.3%. Inversely,  $\epsilon_y$  decreased by more than 39% when moving towards the innermost layer. Such differences may imply a way to equilibrate the high failure strain and the larger drawing zone observed at innermost layers when compared to outermost ones.
- Such variances need to be explained from the characterization of strained polymer layers (outermost, middle and innermost) as they undergo significant volume changes caused by localized polymer chain transformations that disturb the polyethylene semi-crystalline structure. In literature, it is proposed that spherulitic crazing, tie-molecules and cavitation mechanisms are behind the heterogeneous behavior of layers across the pipe wall during extrusion and cooling stages.
- The proposed grooving procedure and the established filament testing protocol are found to be suitable to investigate mechanical heterogeneities and quantify the associated variances. Also, structural analyses can be carried out at very localized points or layers within the pipe wall.

### Acknowledgements

Part of this research is achieved within the 2019 PRFU project: "Mechanical behavior and remaining life of HDPE pipes subjected to operating and environmental conditions" (Code A11N01UN230120190008). The authors are grateful to the Algerian Ministry of Higher Education and Scientific Research (DGRSDT-MESRS), the National Higher School of Mining and Metallurgy (Annaba) and the CRTI (Annaba). Commitment, investment and persistence in laboratory work of one author (Mrs. S. Mammeri) for the accomplishment of this research are highly praised. Fruitful discussions with lab researchers, master students (M2) and lab staff are very appreciated (Dr L. Alimi, Dr N. Hamlaoui, C. Djendi, F. Zoghba, A. Guenouche, I. Lalaymia, and A. Aoussat).

### Nomenclature:

ap:	Depth of cut (mm)
DL:	Degrees of freedom
$f$ :	Feed rate (mm/rev)
F:	Fisher test
HDPE:	High Density Polyethylene
L:	Filament height bend (or curvature) (mm).
P:	Error value compared at 5%
PE:	Polyethylene
P-value:	Probability value
R <sup>2</sup> :	Determination coefficient
R <sup>2</sup> Adjusted:	Response % variation explained by the model
Ra:	Arithmetic mean roughness ( $\mu\text{m}$ )
RSM:	Response Surface Methodology
Rt:	Total roughness ( $\mu\text{m}$ )
SDR:	Pipe diameter to thickness ratio (Standard Dimension Ratio)
T:	Temperature ( $^{\circ}\text{C}$ )
Vc:	Cutting speed (mm/min)

Greek Letters:

$\alpha$ :	Clearance angle (°)
$\sigma_y$ :	Yield stress (MPa)
$\varepsilon_f$ :	Failure strain (%)
$\varepsilon_y$ :	Yield strain (%)
$\gamma$ :	Rake angle (°)
$\kappa r$ :	Cutting-edge (or steering) angle (°)
$\lambda$ :	Cutting edge inclination angle (°).

References

- [1] PPI, Historical review of pressure rating methods for PE and PEX pipe in gas applications. Technical Report TR-55, 2023, 22.  
<https://www.plasticpipe.org/EnergyPipingSystems/EnergyPipingSystems/Publications/Energy-Technical-PPI-Literature.aspx>
- [2] PPI, Polyethylene Piping Distribution Systems for Components of Liquid Petroleum Gases. Technical Report TR-22, 2013, 7.  
<https://www.plasticpipe.org/common/Uploaded%20files/Technical/TR-22.pdf>
- [3] US Nuclear Regulatory Commission, Review of literature on the use of polyethylene (PE) piping in nuclear power plant safety-related class 3 service water systems. Report to The US NRC under NRC Contract No. DR-04-07-072 EMC2, 2007, 30.  
<https://www.nrc.gov/docs/ML1426/ML14266A208.pdf>
- [4] NESCC, Polymer Piping Codes and Standards for Nuclear Power Plants Current Status and Recommendations for Future Codes and Standards Development, Polymer Piping Task Group, 2013, 70.  
[https://share.ansi.org/shared%20documents/Meetings%20and%20Events/NESCC/NESCC\\_Final\\_Report\\_HDPE\\_Task\\_Group.pdf](https://share.ansi.org/shared%20documents/Meetings%20and%20Events/NESCC/NESCC_Final_Report_HDPE_Task_Group.pdf)
- [5] Alludin M, Choudhury IA, El Badarie MA, Hashmi MSJ. Plastics and their machining: A review. J. Mater. Proc. Technol., 1995; 54(1-4): 40-46.  
[https://doi.org/10.1016/0924-0136\(95\)01917-0](https://doi.org/10.1016/0924-0136(95)01917-0)
- [6] Kaiser MS, Fazlullah F, Ahmed SR. A comparative study of characterization of machined surfaces of some commercial polymeric materials under varying machining parameters. J. Mech. Eng., Automation & Control Syst. 2020;1(2):75-88.  
<https://doi.org/10.21595/jmeacs.2020.21643>
- [7] Carr WJ, Feger C. Ultraprecision machining of polymers. Precision Engineering, 1993; 15(4): 221-237. [https://doi.org/10.1016/0141-6359\(93\)90105-J](https://doi.org/10.1016/0141-6359(93)90105-J)
- [8] Kiass N, Khelif R, Boulanouar L, Chaoui K. Experimental Approach to Mechanical Property Variability through a High-Density Polyethylene Gas Pipe Wall. Journal of Applied Polymer Science. 2005; 97:272-281. <https://doi.org/10.1002/app.21713>
- [9] Kaddeche M, Chaoui K, Yaltese MA. Cutting parameters effects on the machining of two high density polyethylene pipes resins. Mechanics & Industry, 2012;13(5):307-316.  
<https://doi.org/10.1051/meca/2012029>
- [10] Hamlaoui N, Azzouz S, Chaoui K, Azari Z, Yaltese MA. Machining of tough polyethylene pipe material: surface roughness and cutting temperature optimization. Int. J. Adv. Manuf. Technol. 2017;92, 5(8):2231-2245.  
<https://doi.org/10.1007/s00170-017-0275-4>
- [11] Salles JLC, Gonçalves MTT. Effects of machining parameters on surface quality of the ultra-high molecular weight polyethylene (UHMWPE). Materia. 2002;8(1):1-10.
- [12] Xiao KQ, Zhang LC. The role of viscous deformation in the machining of polymers. Int. J. Mech. Sci. 2002;44(11):2317-2336.  
[https://doi.org/10.1016/S0020-7403\(02\)00178-9](https://doi.org/10.1016/S0020-7403(02)00178-9)

- [13] Mammeri S, Chaoui K, Bouacha K. Manufacturing of testing specimens from tough HDPE-100 pipe: Turning parameters optimization, Int. J. Res. Eng. Struct. Mat. (In press, Accepted: Nov., 1st, 2023, Online First).  
<https://doi.org/10.17515/resm2023.38ma0714rs>
- [14] Technical documents on HDPE gas pipes. CHIALI Co., 2023. <https://www.groupe-chiali.com>
- [15] Mammeri S, Bouacha K, Chaoui K. Optimization of HDPE material orthogonal machining. 1st Nat. Conf. on Sci. & Technol., Mascara University, 27-28 June 2023.
- [16] Belhadi S, Kaddeche M, Chaoui K, Yaltese M-A. Machining Optimization of HDPE Pipe Using the Taguchi Method and Grey Relational Analysis. Int. Polym. Process. XXXI 2016;4:491-502. <https://doi.org/10.3139/217.3271>
- [17] Vasques B. Étude du comportement du rayon d'arête et de son influence sur l'intégrité de surface en tournage à sec, Ph.D. Dissertation, Tours Univ., France, 2005.
- [18] Cat. S60 Smartphone, User Manual. Caterpillar, 2016.  
<https://www.catphones.com/download/User-Manuals/S60-Smartphone/S60-User-Manual-English.pdf>
- [19] Mitsubishi Chemical Group. Guide To Machining Plastic Parts, Metric System. Machinist's Toolkit (2023).  
<https://www.mcam.com/mam/41701/MCG-Machinist-Toolkit-A4-EU-metric.pdf>
- [20] Curbell Plastics, Inc. Plastic Turning Machining Guidelines (2003).  
<https://www.curbellplastics.com/services-capabilities/fabrication-machined-parts/plastic-machining-guidelines/plastic-turning-machining-guidelines/>
- [21] Alateyah AI, El-Taybany Y, El-Sanabary S, El-Garaihy WH, Kouta H. Experimental investigation and optimization of turning polymers using RSM, GA, Hybrid FFD-GA, and MOGA Methods. Polymers. 2022;14,3585. <https://doi.org/10.3390/polym14173585>
- [22] Chaoui K, Chudnovsky A, Moet A. Effect of residual stress on crack propagation in MDPE pipes. J. Mater. Sci. 1987;22:3873-3879. <https://doi.org/10.1007/BF01133334>
- [23] Patel Y. The Machining of Polymers. Ph.D. Dissertation, Imperial College London, UK, 2008. <https://spiral.imperial.ac.uk/bitstream/10044/1/4435/1/Patel-Y-2009-PhD-Thesis.pdf>
- [24] Rehab-Bekkouche S, Ghabeche W, Kaddeche M, Kiass N, Chaoui K. Mechanical behaviour of machined polyethylene filaments subjected to aggressive chemical environments. MECHANIKA. 2009;77(3):40-46.
- [25] Ghabeche W, Chaoui K, Zeghib N. Mechanical properties and surface roughness assessment of outer and inner HDPE pipe layers after exposure to toluene methanol mixture. Int. J. Adv. Manuf. Technol. 2019;103:2207-2225.  
<https://doi.org/10.1007/s00170-019-03651-z>
- [26] Djendi C. Étude expérimentale du vieillissement du HDPE dans un environnement de dichlorométhane liquide (DCM) : Analyses de la sorption et des propriétés mécaniques. Master's Thesis, Mech. Eng. Dept., Badji Mokhtar University, Annaba, Algeria, 2023. (in French).
- [27] Almomani A, Mourad AI, Deveci S, Wee JW, Choi B-H. Recent advances in slow crack growth modeling of polyethylene materials. Materials & Design. 2023;227:111720.  
<https://doi.org/10.1016/j.matdes.2023.111720>
- [28] Wang Y, Lin D, Xiang M, Cui M, Liu N. Experimental study on aging performance of polyethylene gas pipelines. 3rd Int. Conf. on Air Pollution & Environmental Eng., IOP Conf. Series: Earth and Environmental Science. 2021;631:012066.  
<https://doi.org/10.1088/1755-1315/631/1/012066>
- [29] Humbert S, Lame O, Vigier G. Polyethylene yielding behaviour: What is behind the correlation between yield stress and crystallinity? Polymer. 2009; 50:3755-3761.  
<https://doi.org/10.1016/j.polymer.2009.05.017>

- [30] G'Sell C, Dahoun A, Royer FX, Philippe MJ. The influence of the amorphous matrix on the plastic hardening at large strain of semicrystalline polymers. *Modelling & Simulation in Mater. Sci. & Eng.* 1999;7(5):817-828.  
<https://doi.org/10.1088/0965-0393/7/5/313>
- [31] Addiego F, Dahoun A, G'Sell C, Hiver JM. Characterization of volume strain at large deformation under uniaxial tension in high-density polyethylene. *Polymer.* 2006;47:4387-4399 <https://doi.org/10.1016/j.polymer.2006.03.093>
- [32] Addiego F, Dahoun A, G'Sell C., Hiver JM, Godard O. Effect of microstructure on crazing onset in polyethylene under tension. *Polymer Eng. & Sci.* 2009;49(6):1198-1205.  
<https://doi.org/10.1002/pen.21194>
- [33] Séguéla R. critical review of the molecular topology of semicrystalline polymers: The origin and assessment of intercrystalline tie molecules and chain entanglements. *J. Polym. Sci. Part B: Polym. Phys.* 2005;43(14):1729-1748.  
<https://doi.org/10.1002/polb.20414>
- [34] Kida T, Hiejima Y, Nitta K-H, Yamaguchi M. Evaluation of microscopic structural changes during strain hardening of polyethylene solids using In situ Raman, SAXS, and WAXD measurements under step-cycle test. *Polymer.* 2022;250:124869.  
<https://doi.org/10.1016/j.polymer.2022.124869>